



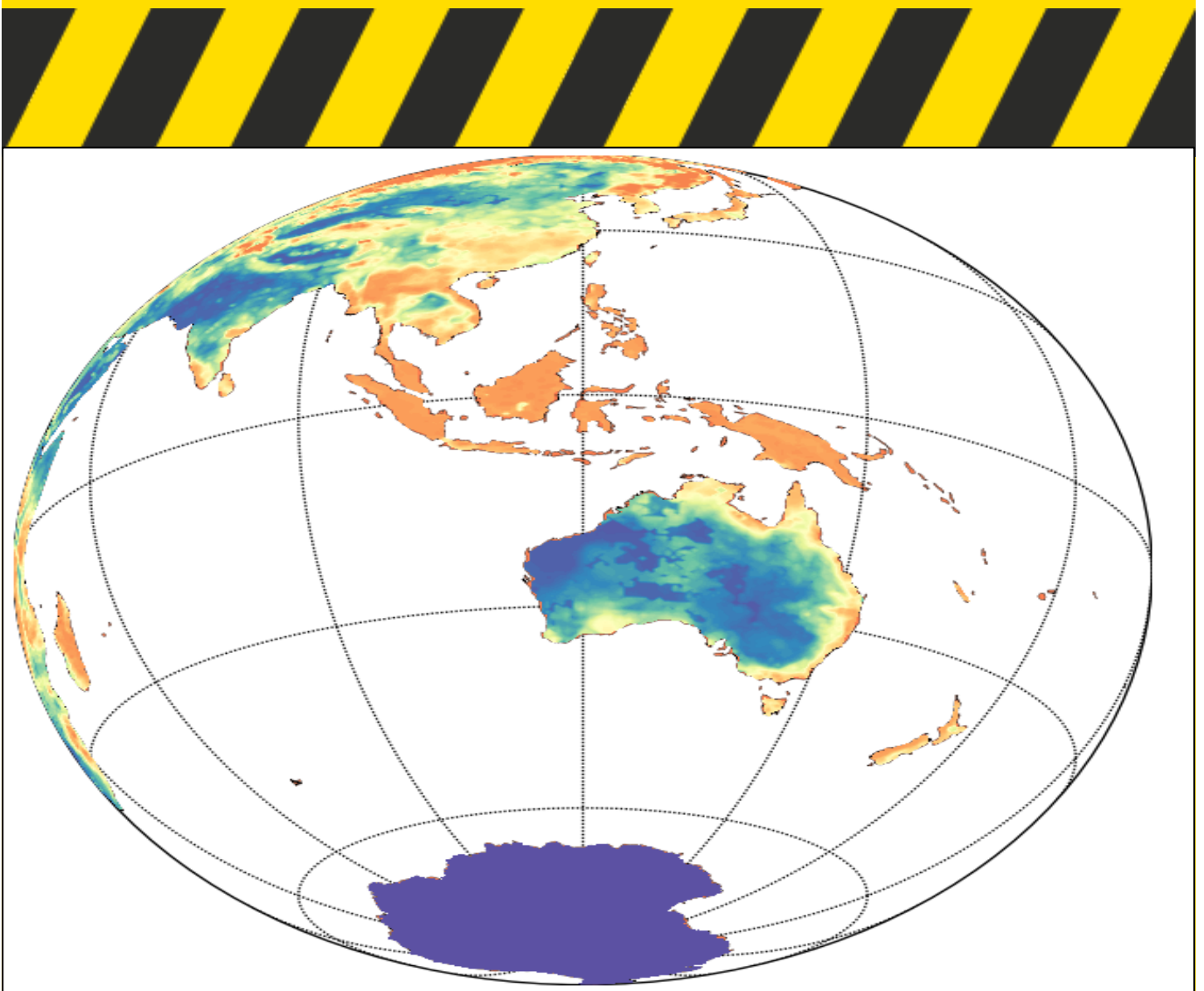
EXPLORING THE SOIL MOISTURE-LIVE FUEL MOISTURE RELATIONSHIP

Vinodkumar^{1,2}, Imtiaz Dharssi^{1,2}, Marta Yebra^{2,3} & Paul Fox-Hughes^{1,2}

¹ Bureau of Meteorology

² Bushfire and Natural Hazards CRC

³ Australian National University





Version	Release history	Date
1.0	Initial release of document	19/06/2020
1.1	Second revision	01/07/2020



Australian Government
Department of Industry, Science,
Energy and Resources

Business
 Cooperative Research
 Centres Program

© 2020 Bushfire and Natural Hazards CRC

All material in this document, except as identified below, is licensed under the Creative Commons Attribution-Non-Commercial 4.0 International Licence.

Material not licensed under the Creative Commons licence:

- Department of Industry, Science, Energy and Resources logo
- Cooperative Research Centres Program logo
- Bushfire and Natural Hazards CRC logo
- All other logos
- All photographs, graphics and figures

All content not licenced under the Creative Commons licence is all rights reserved. Permission must be sought from the copyright owner to use this material.



Disclaimer:

The Bureau of Meteorology, Australian National University and the Bushfire and Natural Hazards CRC advise that the information contained in this publication comprises general statements based on scientific research. The reader is advised and needs to be aware that such information may be incomplete or unable to be used in any specific situation. No reliance or actions must therefore be made on that information without seeking prior expert professional, scientific and technical advice. To the extent permitted by law, the Bureau of Meteorology, Australian National University and the Bushfire and Natural Hazards CRC (including its employees and consultants) exclude all liability to any person for any consequences, including but not limited to all losses, damages, costs, expenses and any other compensation, arising directly or indirectly from using this publication (in part or in whole) and any information or material contained in it.

Publisher:

Bushfire and Natural Hazards CRC

October 2020

Citation: Kumar V, Dharsai I, Yebra M & Fox-Hughes P (2020) Exploring the soil moisture-live fuel moisture relationship, Bushfire and Natural Hazards CRC, Melbourne.

Cover: Soil moisture from ACCESS global numerical weather prediction model.



TABLE OF CONTENTS

ABSTRACT	3
INTRODUCTION	4
DATASETS	6
JASMIN	6
Live fuel moisture content	6
METHODS, RESULTS AND DISCUSSIONS	7
Location-based analysis	7
LMFC predictive model	11
CONCLUDING REMARKS	15
ACKNOWLEDGEMENTS	17
REFERENCES	18



ABSTRACT

Live fuel moisture content is a key factor that determines the flammability of vegetation in ecosystems. Prediction of live fuel moisture content is inherently a very difficult problem since it is modulated by the complex physiological, phenological and ecological processes characteristic of the plant species. Soil moisture is one of the key variables that is known to influence plant water use. Recently, a new live fuel moisture content near-real-time product has been developed for Australia using a radiative transfer model inversion technique on the MODerate Resolution Imaging Spectroradiometer reflectance data. This live fuel moisture content product forms the basis of the Australian Flammability Monitoring System. At the same time, an advanced soil moisture analysis system has been developed by the Bureau of Meteorology recently, called the Joint United Kingdom Land Environment Simulator based Soil Moisture Information (JASMIN). JASMIN can estimate soil moisture at 5 km resolution on a daily timestep for the whole of Australia.

The present study brings together the above two products and explores the live fuel moisture content–soil moisture relationship on a national scale. This study will report the preliminary work carried out in understanding live fuel moisture content–soil moisture relationship and suggests an approach that may be constructive in advancing the ability to predict live fuel moisture content reliably to support fire management. A preliminary analysis is being conducted over 60 selected locations where JASMIN is found to have good skill. These 60 sites together represent a range of land cover types and climate zones typical of the Australian landscape. All the possible soil moisture profiles that can be derived from the four JASMIN soil layers are used for the analysis. Lag-correlation analysis shows that the strength of the relationship between live fuel moisture content and soil moisture varies from site to site and in general, is moderately strong (median lag-correlation of ~ 0.5). However, the strength of the relationship varies with vegetation type and also with soil profile depth. At all the sites, soil moisture is found to be an (important) leading indicator of live fuel moisture content. The lag also varies with the location and is found to range from days to months. Except for the forested sites, the top two soil layers exhibit a higher correlation with live fuel moisture content compared to the deeper layers. We develop a simple model to predict live fuel moisture content. The model is found to have good skill with an average R^2 of 0.64 over the 60 sites. The normalized root mean square error for the model prediction is found to be less than 25% in general.



INTRODUCTION

Fuel moisture content (FMC) is a critical variable affecting fire interactions with fuel and partly controls the efficiency of fire ignition and burning. For example, Dowdy and Mills (2012) showed that FMC influences the risk of ignition from lightning in south-east Australia. The moisture content of dead fuel (forest leaf litter, twigs etc.) is found to be dependent on the atmospheric variability (Viney, 1991) and can be modelled reasonably well using weather variables (Matthews, 2013). However, the moisture content of live vegetation is more complicated because it depends on eco-physiological properties that may significantly vary among different plant species (Pellizaro et al., 2007). The living vegetation may act as a heat source or a heat sink, conditional to the moisture content and the fire heat flux, and thereby either contributing to or inhibiting fire propagation and intensity (Nelson, 2001).

Live fuel moisture content (LFMC) is defined as a ratio of the mass of water contained within vegetation to that of dry mass, expressed as a percentage (Yebra et al., 2019). LFMC variations are related to both environmental conditions (e.g. meteorological variables, soil water availability) and eco-physiological characteristics of the plant species (Castro et al., 2003). Research has shown that LFMC can be derived with good accuracy on a continental scale using measurements from optical remote sensing-based satellite platforms (Yebra et al., 2018). Such a product not only offers the large-scale observability but also provides a much higher temporal and spatial resolution compared to the point-based, weekly-monthly resolution typical of the traditional, manual observing methods. Recently, a new LFMC near-real-time product has been developed for Australia using a radiative transfer model inversion technique on MODerate resolution Imaging Spectroradiometer (MODIS) reflectance data (Yebra et al., 2018). This LFMC product forms the basis of the Australian Flammability Monitoring System (AFMS), a web-based interface monitoring the LFMC routinely across the landscapes (<http://anuwald.science/afms>).

Optical remote-sensing based LFMC products, however, lack the predictive capability desirable for fire management. Also, the sampling density is limited by the satellite over-pass frequency and cloud-cover. Therefore, it is desirable to have models that could reasonably predict the LFMC from more easily accessible parameters. The soil moisture (SM) state is a key factor in assessing the dryness of vegetation due to the relationship that exists between the two variables (Burgan, 1988; Viegas et al., 1992). The Keetch-Byram Drought Index (KBDI), which measures cumulative soil water deficit in forested ecosystems is found to exhibit a strong relationship with LFMC (Dimitrakopoulos and Bemmerzouk, 2003). There are a variety of indices in use across the world which estimate SM as a proxy for land dryness and can be related to LFMC. For example, Viegas et al. (2001) and Castro et al. (2003) found that a non-linear relationship can be derived between moisture codes in the Canadian Forest Fire Weather Index (FWI) system and LFMC data for Mediterranean vegetation.

Although estimating the soil moisture deficit indices using meteorological data is relatively easy to achieve, there are a few issues in using them to model LFMC. First, drought indices are traditionally computed at point locations and may not be representative of larger areas. Secondly, these indices are rather simplified,



empirical, water balance models that do not consider most factors that influence SM dynamics. For example, the KBDI and Soil Dryness Index (SDI) methods used operationally in Australia neglect spatial variations in soil type, vegetation type, terrain and aspect. The above indices also over-simplify evapotranspiration and runoff processes, potentially leading to large errors in estimated SM state. Studies have shown that SM from land surface models is more accurate than the above indices (Vinodkumar et al., 2017). Hence, efforts were made to develop a prototype system based on Joint UK Land Environment Simulator (JULES) land surface model (LSM) to estimate soil moisture deficit for fire danger rating (Dharssi and Vinodkumar, 2017). This system, called the JULES based Australian Soil Moisture Information (JASMIN), estimates SM at a spatial resolution of 5 km for the whole of Australia. Verification against ground-based SM observations shows that a prototype version of this system is significantly better than the KBDI and SDI models (Dharssi and Vinodkumar, 2017). SM is not a direct input in fire danger calculations in Australia. Holgate et al. (2017) proposed that the fuel availability measure in McArthur's Forest Fire Danger Index (FFDI) could entirely be replaced with SM alternatives, but the recalibration of the FFDI to actual bushfire conditions would be required to be accepted operationally. Consequently, there is a need to determine how SM can be integrated effectively into existing fire danger rating systems to facilitate greater use of SM information in fire management and its relation to fuel moisture conditions.

The present study aims to combine the AFMS-LFMC and JASMIN-SM dataset to conduct some preliminary investigation on the suitability of SM as a predictor for LFMC. Our research aims to determine the strength of the relationship between LFMC and SM over the Australian landscape. The study also aims to develop a simple model to predict LFMC changes using SM estimates. An understanding of the complex live fuel – soil moisture content relationship can help in designing operational fire behaviour forecasting models.



DATASETS

JASMIN

The JASMIN system runs at 5 km resolution with an hourly time interval (Dharssi and Vinodkumar, 2017). The soil column extends from the surface to 3 m and is divided into four layers of thickness 10 cm, 25 cm, 65 cm and 200 cm. JASMIN is driven mainly by observation-based analyses based on various Bureau of Meteorology (BoM) systems. The BoM's Mesoscale Surface Analysis System (MSAS; Glowacki et al., 2012) data is used to provide the JULES driving data for air temperature, specific humidity, wind speed and surface pressure. The downward surface solar radiation data is from a near-real-time BoM product derived from the Himawari Geostationary Meteorological Satellites and is available at about 5 km resolution. The downward surface longwave radiation data is obtained from BoM's regional numerical weather prediction model at 12 km resolution (Puri et al., 2013). Rainfall data is from the Australian Water Availability Project (AWAP; Jones et al., 2009) and available as daily accumulations. Tropical Rainfall Measuring Mission (TRMM; Huffman et al., 2007) data is used to disaggregate AWAP rainfall to 3-hourly values. The disaggregation methodology is part of the JULES modelling framework (Williams and Clark, 2014). The TRMM data is also used to fill spatial gaps in AWAP data.

LIVE FUEL MOISTURE CONTENT

The LFMF data is derived by using a radiative transfer model inversion technique on the MODIS reflectance data (Yebra et al. 2018). First, three different radiative transfer models, one for each fuel type, are used to simulate reflectance spectra for the moisture content range for three fuel types (grasslands, shrublands and woodlands/forest). These simulated spectra are then used as reference lookup tables to map the corresponding LFMF values from the quality-controlled observed MODIS reflectance data of the day. MODIS land cover maps are used to identify the dominant fuel type corresponding to each pixel. The MODIS reflectance and land cover data are at 500 m resolution resulting in LFMF retrievals of 500 m spatial resolution every four days. The methodology used to map FMC in Australia is based on previous experience in retrieving FMC in Europe (Jurdao et al. 2013; Yebra and Chuvieco 2009a, b). Existing field LFMF data collected in grassland, shrubland and forest between 2004 to 2014 were used to validate the algorithm retrievals (Yebra et al., 2018).

METHODS, RESULTS AND DISCUSSIONS

LOCATION-BASED ANALYSIS

Our approach is to first evaluate the relationship between the two variables at selected locations which sample the climatic zones and vegetation types typical of the Australian landscape. In that respect, we analyse the datasets over three well-known SM networks, named CosmOz, OzFlux and OzNet (Figure 1). The three networks together comprise of about 60 sites spanning across the whole country. Another reason to select these locations is the demonstrated skill of JASMIN at these sites (Vinodkumar and Dharssi, 2019).

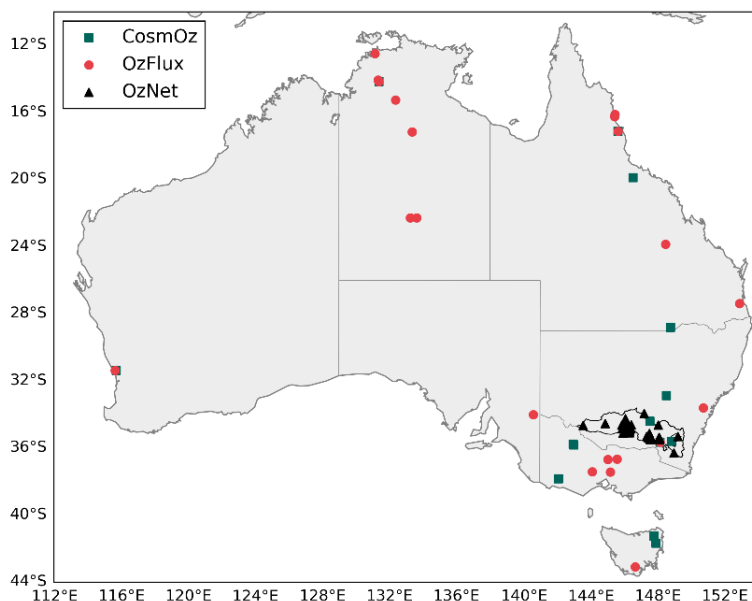


FIGURE 1. SITES OVER WHICH THE LOCATION-BASED ANALYSIS OF LFMC AND SM IS CARRIED OUT. THE LOCATIONS CORRESPOND TO THE THREE IN SITU SOIL MOISTURE NETWORKS – COSMOZ (GREEN SQUARE), OZFLUX (RED CIRCLE) AND OZNET (BLACK DIAMOND).

The location-based analysis is conducted for a period spanning from 2010 to 2019. The JASMIN SM analysed here is in volumetric units ($m^3 m^{-3}$). The data at each location is collocated using the nearest-neighbour approach. In general, LFMC displays a strong seasonality where the values typically reach their lowest before the seasonal rains have commenced. This annual cycle is illustrated through the time series plot over Baldry in the southern tableland region of New South Wales (black, dotted line; Figure 2). The Baldry site is part of the CosmOz network with the land classified as a mix of pasture and reforested woodland. The site is situated in a semi-arid environment with annual rainfall dominated by winter precipitation produced by mesoscale extra-tropical disturbances. The LFMC time series over Baldry shows peaks after the wet season and the vegetation gradually drying out into the drier summer months. The site also displays short-lived spikes after significant rain events, highlighting that the plants can utilize moisture transported into the shallow soil layers after a rain event.

JASMIN has four soil layers and it is not precisely clear which of these layers best represents the root zone at a given location. The top two layers are often found to be influenced by weather events characterized by sharp wetting and drying phases. The temporal dynamics of these two layers at Baldry typify the widely



occurring pattern across the landscape (Figure 2). Temporal variations in the 35-100 cm layer are less sizable and rather smooth compared to the two layers over it. This deepest layer is less influenced directly by what happens at the surface as the top two layers act as a natural filter in modulating the water transport downwards. The bottom-most soil layer in JASMIN is even less dynamic due to the depth and thickness of the layer. In general, the bottom two layers show similar temporal characteristics across locations as well. There is a visible hysteresis and only the significant and persistent rain events recharge the bottom layers.

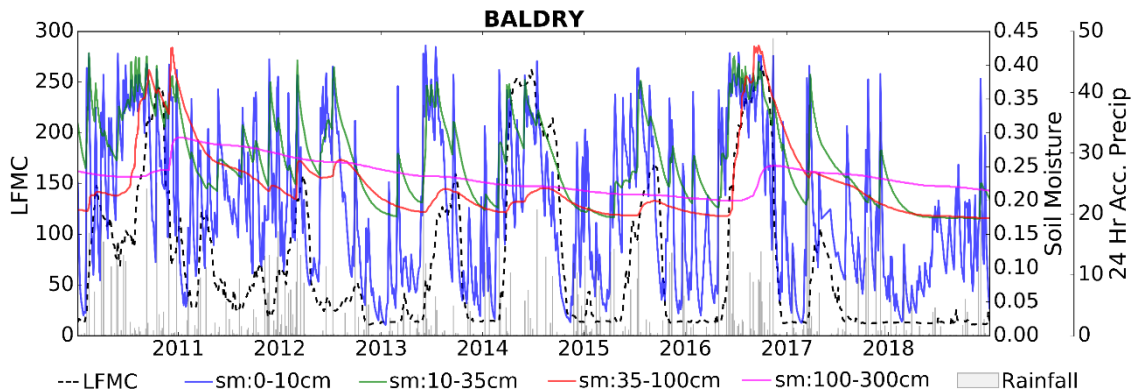


FIGURE 2. TIME SERIES PLOTS OF LFM, SM AND 24-HOUR ACCUMULATED RAINFALL OVER THE BALDRY SITE IN NEW SOUTH WALES (MIX OF PASTURE AND REFORESTED WOODLAND). LFM DATA IS FROM THE AFMS, SM FROM THE JASMIN AND RAINFALL FROM THE AWAP. SM FROM ALL FOUR SOIL LAYERS IN JASMIN IS SHOWN AND IS PRESENTED IN VOLUMETRIC UNITS ($M^3 M^{-3}$).

A lag-correlation analysis is conducted between LFM and SM from all the native JASMIN layers and the combination of layers that can be rationally derived using the four native soil profiles (using weighted average based on layer depth). The results presented in Figure 3 depict the maximum lag-correlation and the corresponding lag (in days) for each site. The skill scores are segregated into four broad land cover types. The land cover classification is made based on the information from *in-situ* locations. The results indicate that the strength of the relationship between LFM and SM varies from site to site. The observed variation in the correlation can be caused by a variety of factors, including spatial variability in plant type, physiology and morphology, climate, soil properties and depth. The range in lag time indicates that there is a significant difference in the physical processes happening at each location, from the transport of water through the soil from the surface to the root-zone and the eventual uptake of moisture by plants.

The present study aims to develop a simple model to explain the relationship between LFM and SM. In that respect, we prefer to use a single SM profile as the predictor for LFM. From our analysis, we identify soil moisture content from the 0-35 cm profile (SM_{0-35cm}) provides the best skill in terms of the correlation with LFM. The SM_{0-35cm} displays a strong relationship with the LFM at different land cover types. One possible reason for this larger degree of agreement is that both the SM_{0-35cm} and LFM exhibits strong seasonality. The deeper layers may not always display the strong seasonality exhibited by the shallower layers. Besides, the deeper layers may miss the short-term variations associated with individual weather events to which the plants and shallow soil profiles respond. Also, the upper and deeper soil layers can be disconnected in land surface models due to uncertainties in the parameterizations. This may result in deeper layers exhibiting little seasonality, rendering them less useful to predict



season-al LFMC changes. This also gives rise to artificial correlations at a longer time lag, as evident from the box and whisker plots for the 100-300 cm profile (Figure 3).

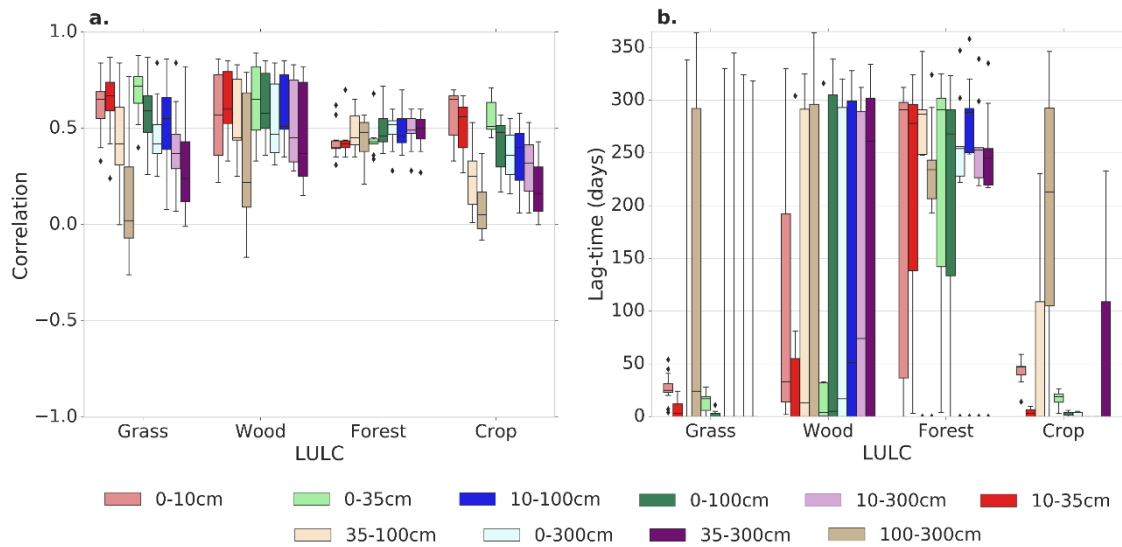


FIGURE 3. BOX AND WHISKER PLOT REPRESENTING A) LAG-CORRELATION AND B) LAG IN DAYS BETWEEN LFMC AND SM FROM VARIOUS JASMIN NATIVE AND DERIVED LAYERS. THE GROUPING IS DONE BASED ON THE LAND-USE/LAND -COVER (LULC) TYPE OF THE OBSERVING SITE. THE OUTLIERS ARE MARKED AS DIAMONDS.

In general, a strong linear relationship is found between the LFMC and SM_{0-35cm} , except for forested locations (Figure 3). The average maximum lag-correlation observed for grasslands, woodlands, forestlands and croplands between LFMC and SM_{0-35cm} are 0.71, 0.69, 0.47 and 0.5, respectively. The corresponding average lag is 14.28, 64.54, 218.91 and 16.85 days. The forested sites generally display a stronger correlation to the thicker, 0-300 cm soil profile. This is likely a consequence of the deeper roots typical of over-story forest canopies which can draw water from a much thicker soil profile than the 0-35 cm layer. The skill lost by using the 0-35cm profile instead of the 0-300 cm is 0.02 (0.09) in terms of mean (median) correlation.

The association of SM_{0-35cm} to LFMC exhibits very different behaviour for different land cover types as indicated by the correlation analysis. This is suitably illustrated by the frequency histogram of normalized SM_{0-35cm} and LFMC for grassland and evergreen broadleaf forest land cover types over locations and periods where a fire is detected (Figure 4). The normalization scales the volumetric data between (0, 1) using the minimum and maximum values from the respective time series. Thus, the normalization gives a "relative" SM field which represents the "fraction of full wetness" and is often called simply soil wetness (SW) in the literature (Vinodkumar et al., 2017). The occurrence of fire is identified using the MODIS fire radiative power (FRP) data. FRP estimates are available with every active fire pixel reported in the MOD14 and MYD14 fire products derived from the MODIS instrument onboard Terra and Aqua satellites (Giglio et al., 2016). The MODIS FRP retrieval is based on the relationship between the emitted fire energy and infrared brightness temperature estimates in the 4 μm region (Kaufman et al., 1998). The algorithm is valid for FRP retrievals of fires with flaming temperatures greater than 600 K and occupying a pixel fraction less than 0.1 (Wooster et al., 2003). The FRP is given in a unit of megawatts (MW) per pixel. Only pixels with FRP > 50 MW are selected. The evaluation against FRP is carried out for the January

2010 – October 2016 period. The land cover classification is made based on the 500 m resolution MODIS land cover land use type dataset (Broxton et al., 2013).

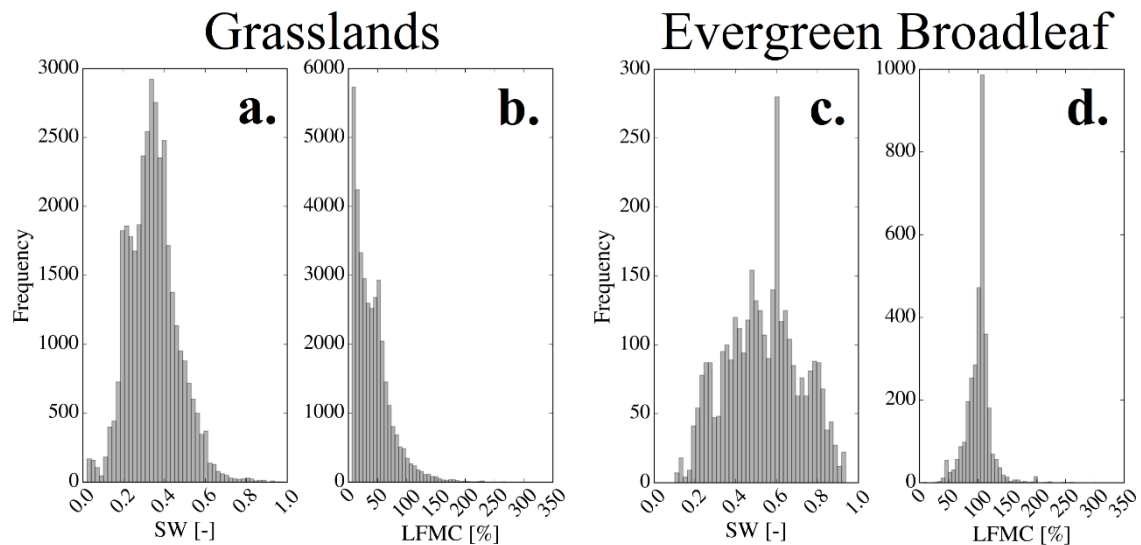


FIGURE 4. FREQUENCY OF SW FROM 0-35CM PROFILE AND LFM OVER GRASSLANDS (A & B), AND EVERGREEN BROADLEAF FORESTS (C & D) RESPECTIVELY. EACH DATA POINT CORRESPONDS TO THE LOCATION IDENTIFIED AS FIRE HOTSPOTS BY THE MODIS FRP DATA COVERING THE WHOLE AUSTRALIA.

Over grasslands, 90% of fire occurs when the SW is ≤ 0.5 (Figure 4a). Some of the highest FRP values (≥ 1000 MW) corresponds to very dry soils (SW < 0.25 ; results not shown). Also, $\sim 93\%$ of fires occur over grasslands when the LFM is $< 100\%$ (Figure 4b). The relationship is found to be more complicated for the evergreen forest sites (Figure 4c). Here, about 56% of total fires are found to occur over wetter soils (SW > 0.5) and only the remaining 44% of fires occur when SW < 0.5 (Figure 4c). The drier soils under grassland, compared to the forest, may reflect the fact that the soil water uptake in grasses is higher than that in woody vegetation (Köchy & Wilson 2000). This is facilitated by higher (~ 20 times) fine root lengths in grassland soils than in forest soils (Jackson et al. 1997). Besides, the root-shoot ratio is nearly 30 times greater in grassland than forest (Wilson 1993). Further, additional factors may lower SM temporal variability in the forest including, reduced evaporation due to lower temperature, reduced wind speed, and larger water holding capacity of clayey soils characteristics of forested sites.

Similar to grassland, the most intense fires (FRP > 1000 MW) over evergreen broadleaf forests are found to occur when SW < 0.5 (figure not presented for brevity). These forested trees can hold water equivalent to its dry weight, even during periods conducive to fires. This is evident from the frequency distribution of LFM where a large proportion of fires occur when LFM is around 100% (Figure 4d). The LFM at these sites seldom falls below 50% in the event of a fire occurring (Figure 4d). The evergreen trees are found to have high wood density and hence can store a substantial amount of water in the stem (Kenzo et al., 2017). Also, the development of deep roots and subsequent water uptake from deeper soil layers are found to be an important strategy enabling evergreen species to overcome seasonal water limitations (Hasselquist et al., 2010). The average root depth in evergreen forests is estimated to be about 3.1 m (Yang et al., 2016). The low correlations observed over forested sites (Figure 3a) is possibly a result of these drought-resistant strategies adopted by the particular vegetation types.



LMFC PREDICTIVE MODEL

The study aims to construct a simple model for predicting LFMC using the gridded JASMIN SM product. The strength and lag of the LFMC and SM relationship are found to vary spatially. The LFMC, in general, is influenced by a variety of factors other than soil moisture availability, including plant physiology and evapotranspiration (Qi et al. 2012). This possibly explains the somewhat different annual cycles exhibited by LFMC to SMC_{0-35cm} (Figure 5). Hence, it is important to address some of these factors implicitly to derive a skilful model for LFMC based on SM. We adopt a modelling strategy similar to that discussed in Fovell et al. (2015), where the LFMC is predicted using a linear combination of an annual cycle model and a model to predict daily deviations from the annual cycle. The annual cycle for both LFMC and SM is constructed separately as a function of time. We select the 0-35 cm profile from JASMIN to model LFMC. The daily deviations in LFMC are predicted using that in SMC_{0-35cm} , where the daily departures are calculated by removing the respective annual cycles from each dataset.

The LFMC data is about 10 times finer than the JASMIN data. To develop the predictive model, the LFMC data is upsampled to 5 km resolution by taking an average of the LFMC values that are encompassed within each JASMIN pixel. The annual model for both LFMC and SMC_{0-35cm} is based on a Fourier cosine series approximated to the 12th harmonics, where day-of-the-year is used as the predictor variable. This simple function is capable of estimating fairly odd-shaped annual cycles in both datasets, an example of which is shown in Figure 5. For a sufficiently long time series, the annual cycle can be computed by just taking the climatological mean for each day. This is not possible here due to the shorter time series. This is even more problematic for LFMC, given the infrequent temporal sampling due to satellite over-pass interval and cloud cover.

The annual cycle of both LFMC and SMC_{0-35cm} varies from location to location and hence each station has a unique function. When the reference AFMS LFMC time series is compared to the annual model for the period extending from January 2010 through December 2019, a sizable 49% of the reference series' variance is captured by the annual model, where the value represents the average for the 60 stations examined. Similarly, for the SMC_{0-35cm} , the average variance that can be explained by the annual model is found to be 37%.

The SM departures are generally found to have good agreement with the LFMC departures. This is illustrated in Figure 6, where a direct comparison is facilitated by superimposing the two residual time series over Baldry in New South Wales. However, it is readily apparent that there is a systematic phase difference between the two residual time series. A lag-correlation analysis for the residuals returned the highest correlation of 0.72 for a lag of 22 days over Baldry. This result further suggests that LFMC is responding directly and strongly to SMC_{0-35cm} changes and the lag signifies the combined time taken for the rainfall received at the surface to percolate through the 0-35 cm layer and the subsequent water uptake process by the plant to occur. The lag between the two residual time series is found to vary from location to location, with a minimum of 0 and a maximum of 29 days.



To keep the predictive model simple, we identified a lag of 14 days as a good compromise to obtain a reasonable linear relationship between the two residual time series at all locations. An ordinary least square regression model with the residual SMC_{0-35cm} as the independent variable to predict daily changes in LFMC is developed for each grid point. The final predictive model is thus constructed using a linear combination of the time function model to predict the annual cycle and the ordinary least square regression model to estimate the daily variations. The predictive model returned an average R^2 of 0.64 over the 60 sites for the training period (2010-2019). The skill varies with location and is found to be lower over locations which have larger temporal variability in either LFMC or SMC_{0-35cm} series.

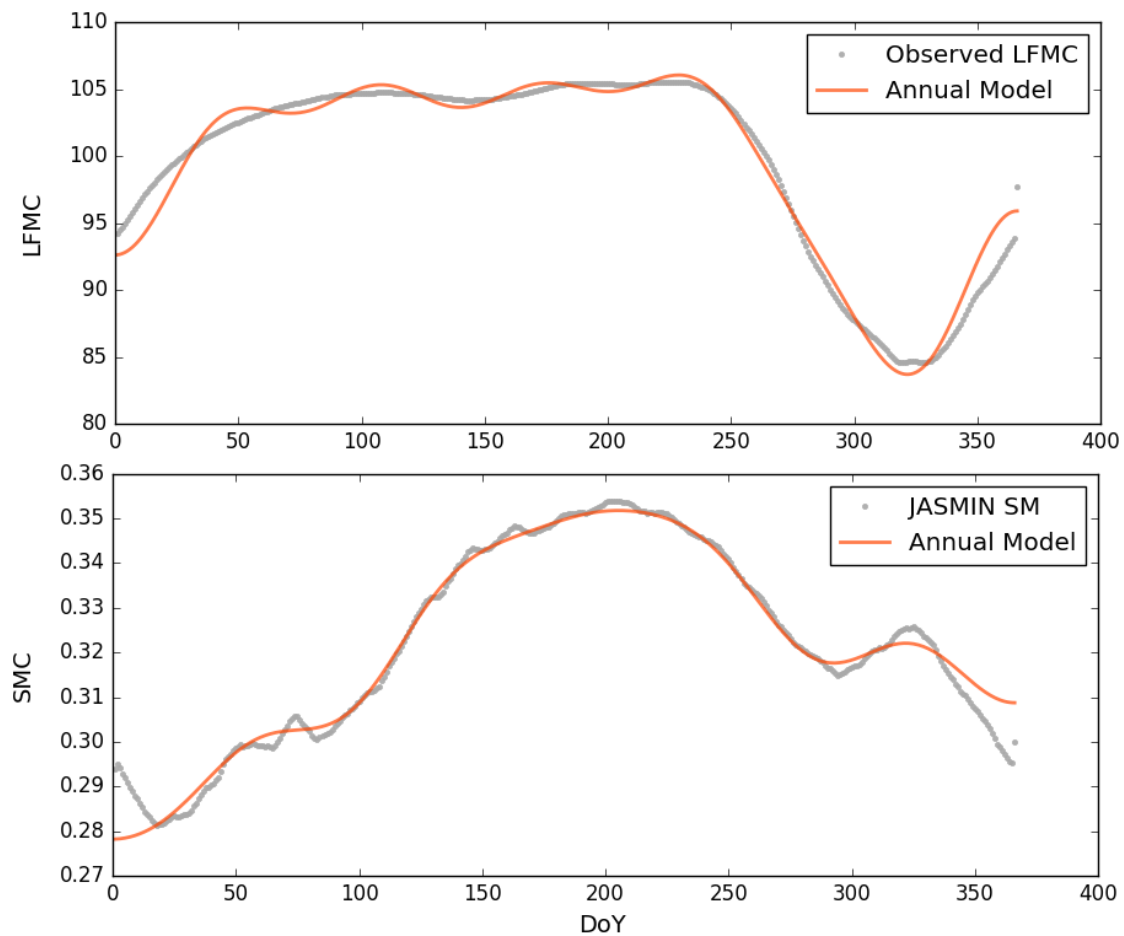


FIGURE 5. OBSERVED (GREY LINE) AND MODELLED (ORANGE LINE) ANNUAL CYCLES OVER TUMBARUMBA, NSW FOR A) LFMC AND B) SMC_{0-35cm} .

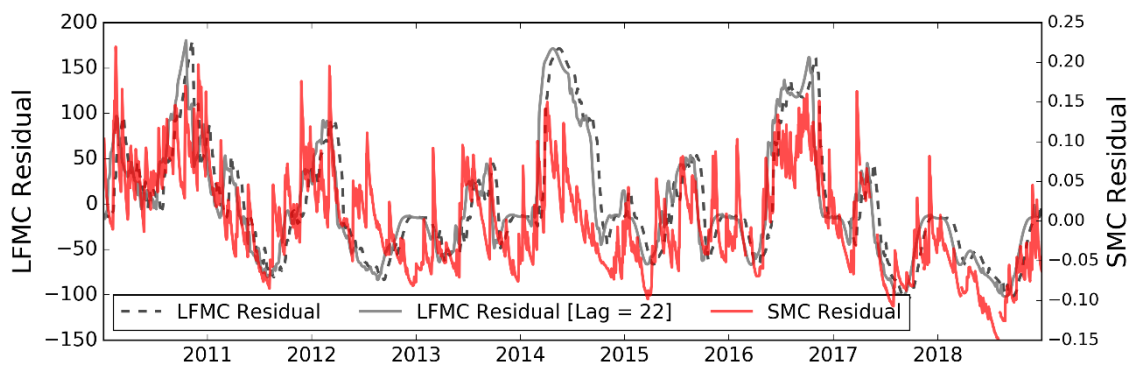


FIGURE 6. RESIDUAL TIME SERIES OF SMC_{0-35cm} (RED LINE) AND LFMC (BLACK BROKEN LINE). THE GREY SOLID LINE CORRESPONDING TO THE LFMC SHIFTED BACKWARD FOR 22 DAYS.



The model is applied to the whole of Australia. The time function model to estimate the annual cycle and the ordinary least squares regression model to estimate the daily variations are computed for each grid point. These two sub-models are then combined linearly to estimate the LFM value at each JASMIN grid point. To check the adequacy of the predictive model, correlation, bias and normalized root mean squared difference (NRMSD) are computed against the original AFMS dataset for the training period (2010 – 2019). The NRMSD score is computed by normalizing the RMSD using the range of the measured LFM. The spatial distribution of the resultant correlation and NRMSD scores are presented in Figure 7. A strong correlation is observed over the tropical, northern savannas and southern grasslands and croplands (Figure 7a). The model is found to be generally unbiased (not shown). The random error in the model is usually less than 25% of the dynamic range as indicated by the NRMSD score (Figure 7b).

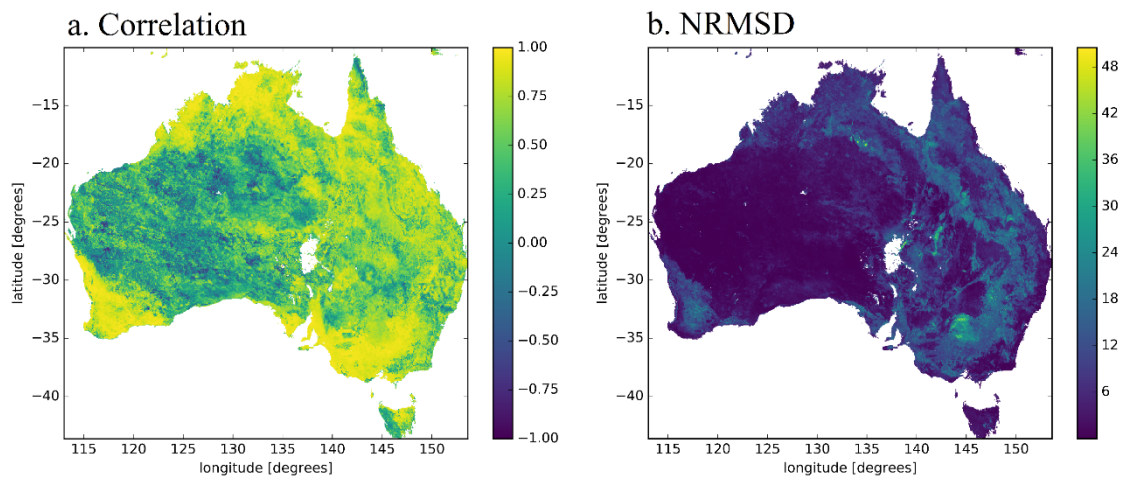


FIGURE 7. VALIDATION OF THE LFM PREDICTIVE MODEL: A) PEARSON'S PRODUCT-MOMENT CORRELATION, AND B) NORMALISED RMSE

The evaluation of the model is extended by comparing the original LFM and modelled LFM against the MODIS FRP data are presented in Figure 8. A log₁₀ transformation is applied to the FRP data. The plots correspond to four land-cover types: grassland (Figure validation 8a), woody savanna (Figure 8b), cropland (Figure 8c), and evergreen broadleaf forest (Figure 8d). For the original AFMS dataset, the mean and standard deviation of LFM over grassland, cropland, woody savannas, and evergreen broadleaf forests when a fire is detected (using MODIS FRP data) are 40.7 ± 30.2 , 78.4 ± 36.1 , 53.9 ± 14.1 , and 101.5 ± 20.3 , respectively. The corresponding scores from the predictive model are 46.2 ± 28.9 , 82.4 ± 30.9 , 58.5 ± 13.3 , and 102.3 ± 17.6 , respectively. The model is found to capture the distribution of the original (AFMS) LFM product in general. The skill of the model over woody savannas (Figure 8b) and evergreen broadleaf forests (Figure 8d) are found to be particularly good.

The model predictions are verified over 6 months from January – June 2020, which falls outside the training data period. Figure 9 depicts the temporal correlation and NRMD obtained from this verification. Only locations where correlations with p-values < 0.05 are shown. The predicted LFM shows a strong correlation in general and especially over the eastern and northern Australia. There are, however, regions that display weaker correlation. This is quite noticeable over the evergreen forest over the south-eastern Australia where the model is found to have low skill. Weaker correlations are also observed over

regions classified as open shrubland typical of central and north-western Australia. However, these results should be understood with a degree of caution as the verification presented here is based on limited sample size. The number of temporal data points varies with location and the maximum sample size available is 38. We acknowledge that this is rather a small sample size to derive spatially consistent skill score. The trade-off is to reduce the training period from 9 years which may lead to a less optimal model fit and hence undesirable. However, this leaves us with a limited sample size for verification. One approach to overcome the limited sample size is to apply a bootstrapping or cross-validation approach. However, this is outside the scope of the present study and will be addressed in future studies.

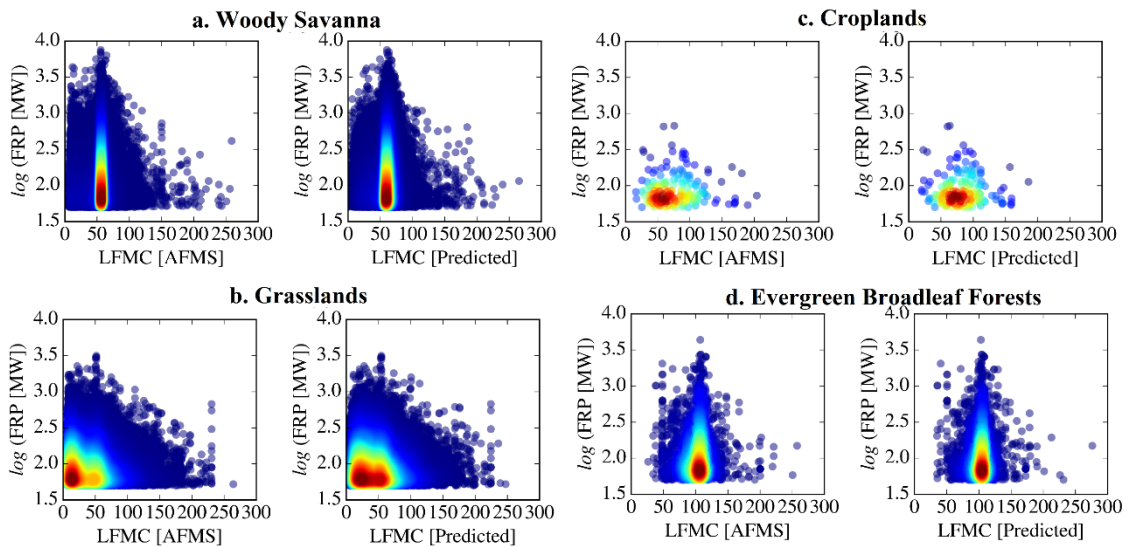


FIGURE 8. Scatter plot of original AFMS LFCM and predicted LFCM against the MODIS FRP. The colours depict the probability density estimated using Gaussian kernel density estimation method. The light blue colours indicate least dense locations on the plot and the dark red indicate the densest locations.

CONCLUDING REMARKS

In the present study, we explore the relationship between live fuel moisture content and soil moisture content on a national scale. Both variables are widely used in fire management practices - the LFMFC is used often directly and the SM as a proxy for fuel moisture/availability. The two variables represent landscape dryness at different strata and the latter can be a good indicator of the former. Remote sensing techniques now allow sampling LFMFC at a continental scale more regularly, which is impractical using the traditional, manual methods. However, temporal and spatial gaps in remote sensing data exist, mainly due to satellite return time and cloud cover. Our study is a first step towards addressing the limitations of remote sensing techniques in estimating LFMFC and developing a predictive model for operational applications.

The study makes use of readily available gridded LFMFC and SM products from the AFMS and JASMIN systems to identify the functional relationship between SM and LFMFC. The results indicate that SM is a leading indicator of LFMFC. This has significant operational implications as daily variations in LFMFC can be predicted using SM information from JASMIN on a national scale. JASMIN is currently run as a prototype, research system with SM analysis done only near-real-time. However, JASMIN can be extended to produce both real-time analysis and forecasts. The prognostic mode can provide SM forecasts for up to 10 days. The model developed here considers a lag of 14 days between SM and LFMFC. This implies a lead time of 14 days for predicting the LFMFC estimates and a maximum lead time of 24 days for a 10-day SM forecast product.

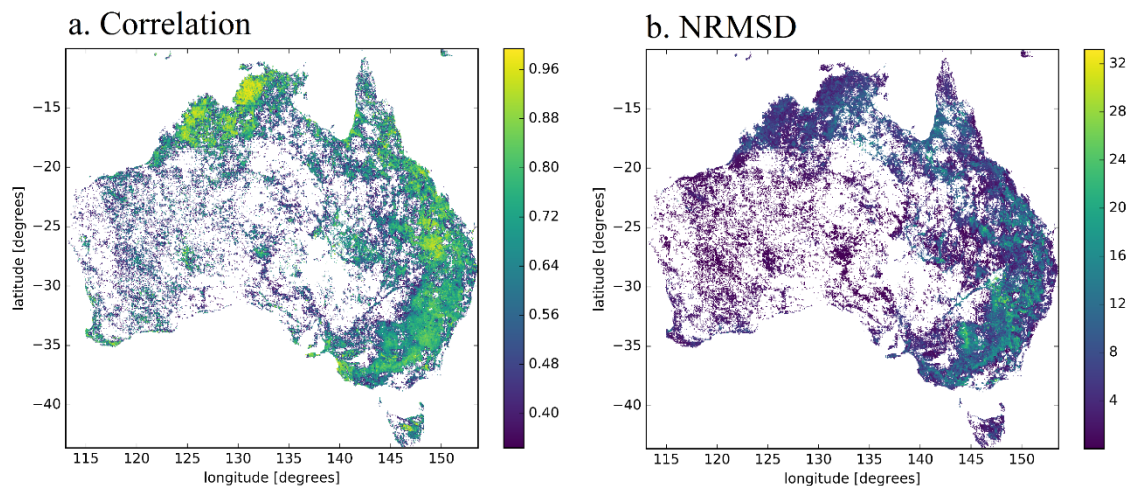


FIGURE 9. PEARSON'S PRODUCT-MOMENT CORRELATION BETWEEN THE ORIGINAL AFMS LFMFC AND THE PREDICTED LFMFC DATASETS. SCORES ARE PRESENTED ONLY FOR LOCATIONS WHERE P-VALUE<0.05.

This preliminary research work was undertaken to understand the relationship that exists between the AFMS LFMFC and JASMIN SM products. In that respect, we kept the modelling strategy fairly simple. For example, the model considers only a single soil profile and lag value at all locations across the country. The correlation analysis indicates that the dependence of LFMFC to SM can vary with vegetation type. For a plant with complex, deeper root systems, the relationship may exist at multiple soil layers. Also, the lag between the two variables is an attribute of the location determined by a range of factors including soil and vegetation characteristics. Therefore, the future modelling strategy may consider a spatially varying lag as well as a combination of soil layers.



We did not consider any noise filtering as a pre-conditioning step to the construction of the predictive model or in the subsequent estimation. It is observed that high-frequency spikes in SM do not match up well with the LFMC data. A temporal average filter applied to the SM time series helps to improve the correlations between the dataset marginally (not presented here). The temporal filter applied to a soil profile is equivalent to expanding the soil horizon downward. At locations where the hydrological coupling between the surface and deeper layers are weak in the model, a temporal filter may help to capture the temporal dynamics of deep layer SM better. However, the time window/parameter(s) for a temporal filter is location specific and should be carefully chosen. The time parameter, in effect, represents all the processes affecting the temporal dynamics of SM, such as the thickness of the soil layer, soil hydraulic properties, evaporation, run-off and vertical gradient of soil properties (texture, density). SM studies have successfully applied an exponential time filter to derive deep layer SM from the near-surface layer SM estimates. Future research may investigate similar methods to address some of the issues arising with the data noise or representative soil depth.

There are other avenues to be explored in the context of using soil moisture information for mapping and predicting fuel conditions. For example, grassland fires are a major threat in the Australian landscape and grass curing is a well-known indicator of fire potential in grassland ecosystems. Studies have shown that LFMC exhibit, in general, exhibits a strong relationship with grass curing (Xuang, 2019). Therefore, the approach discussed in the present study can be extended to identify the relationship between grassland curing and soil moisture. Also, new remote sensing-based techniques are emerging which can characterize the moisture in above-ground biomass. The vegetation optical depth (VOD) information retrieved using microwave radiometry measurements is such a product and is found to be a useful indicator of vegetation water content (Konings et al., 2016). A recent study has assimilated VOD from Soil Moisture Active Passive Mission (SMAP) into a coupled dynamic vegetation - land surface model to assess the impact of 2019 Australian fires on regional water budget (Kumar et al., 2020). This study used NASA's Land Information System (LIS) framework to assimilate the SMAP VOD retrievals. Given that there is a proposal to implement JASMIN within NASA's LIS framework, there is an opportunity to further explore the use of VOD information in JASMIN to map and predict parameters relevant to fire danger in the future. These new products could potentially replace the existing, outdated, fuel availability estimates in fire behaviour models.



ACKNOWLEDGEMENTS

The support of the Commonwealth of Australia through the Bushfire and Natural Hazards Cooperative Research Centre program is acknowledged. We also thank NASA Fire Information for Resource Management System (FIRMS) for the MODIS FRP product. The datasets used in the present study can be accessed using the following the links:

MODIS FRP - <https://firms.modaps.eosdis.nasa.gov/download/>

JASMIN soil moisture -

http://opendap.bom.gov.au:8080/thredds/catalog/c35ee8d2a475e10ea06d0ad53b46ce2a/JASMIN_land_dryness/catalog.html

AFMS LFMC - <http://anuwald.science/afms>



REFERENCES

- 1 Best, M. J., Pryor, M., Clark, D. B., Rooney, G. G., Essery, R. L. H., Menard, C. B., Edwards, J. M., Hendry, M. A., Porson, A., Gedney, N., Mercado, L. M., Sitch, S., Blyth, E., Boucher, O., Cox, P. M., Grimmond, C. S. B., and Harding, R. J., 2011: The Joint UK Land Environment Simulator (JULES), model description - Part 1: Energy and water fluxes, *Geoscientific Model Development*, 4(3), 677–699. doi:10.5194/gmd-4-677-2011.
- 2 Broxton, P. D., Zeng, X., Sulla-Menashe, D., & Troch, P. A., 2014: A global land cover climatology using MODIS data. *Journal of Applied Meteorology and Climatology*, 53(6), 1593-1605.
- 3 Burgan R. E., 1988: Revisions to the 1978 National Fire-Danger Rating System. U.S. Department of Agriculture, Forest Service, South-Eastern Forest Experiment Station: Research Paper. SE-273: Asheville, NC; 39 pp.
- 4 Castro, F. X., Tudela, A., & Sebastià, M. T., 2003: Modeling moisture content in shrubs to predict fire risk in Catalonia (Spain). *Agricultural and Forest Meteorology*, 116(1-2), 49-59.
- 5 Dharssi, I., and Vinodkumar, 2017: A prototype high resolution soil moisture analysis system for Australia, *Bureau of Meteorology Research Report*, No. 026.
- 6 Dimitrakopoulos A. P., and Bemmerzouk A. M., 2003: Predicting live herbaceous moisture content from a seasonal drought index. *International Journal of Biometeorology*, 47, 73–79.
- 7 Dowdy, A.J. and Mills, G.A., 2012: Atmospheric and fuel moisture characteristics associated with lightning-attributed fires. *Journal of Applied Meteorology and Climatology*, 51(11), 2025-2037.
- 8 Fovell, R. G., Rolinski, T., & Cao, Y., 2015: A simple model for the live fuel moisture of chamise, 5.3, 11th Symposium on Fire and Forest Meteorology, Minneapolis, Minnesota.
- 9 Giglio, L., Schroeder, W., & Justice, C. O., 2016: The collection 6 MODIS active fire detection algorithm and fire products. *Remote Sensing of Environment*, 178, 31-41.
- 10 Glowacki, T., Xiao, Y., Steinle, P., 2012: Mesoscale surface analysis system for the Australian domain: design issues, development status, and system validation, *Weather and Forecasting*, 27, 141–157. <https://doi.org/10.1175/WAF-D-10-05063.1> <https://doi.org/10.1175/WAF-D-10-05063.1>
- 11 Hasselquist, N. J., Allen, M. F., Santiago, L. S., 2010: Water relations of evergreen and drought-deciduous trees along a seasonally dry tropical forest. *Oecologia*, 164(4), 881-890. doi:10.1007/s00442-010-1725-y
- 12 Holgate, C. M., van Dijk, A. I. J. M., Cary, G. J., Yebra, M., 2017: Using alternative soil moisture estimates in the McArthur Forest Fire Danger Index. *International Journal of Wildland Fire*, 26, 806-819. doi:10.1071/WF16217
- 13 Huffman, G. J., Bolvin, D. T., Nelkin, E. J., Wolff, D. B., Adler, R. F., Gu, G., Hong, Y., Bowman, K. P., and Stocker, E. F., 2007: The TRMM Multi-Satellite Precipitation Analysis (TMPA): Quasi-Global, Multiyear, Combined-Sensor Precipitation Estimates at Fine Scales, *Journal of Hydrometeorology*, 8(1), 38–55. doi:10.1175/JHM560.1.
- 14 Jackson, R., Mooney, H. A., & Schulze, E. D., 1997: A global budget for fine root biomass, surface area, and nutrient contents. *Proceedings of the National Academy of Sciences*, 94(14), 7362-7366.
- 15 Jurdao, S., Yebra, M., Guerschman, J. P., & Chuvieco, E., 2013: Regional estimation of woodland moisture content by inverting Radiative Transfer Models. *Remote Sensing of Environment*, 132, 59-70.
- 16 Kaufman, Y. J., Justice, C. O., Flynn, L. P., Kendall, J. D., Prins, E. M., Giglio, L., ... & Setzer, A. W. (1998). Potential global fire monitoring from EOS-MODIS. *Journal of Geophysical Research: Atmospheres*, 103(D24), 32215-32238.
- 17 Kenzo, T., Sano, M., Yoneda, R., & Chann, S., 2017: Comparison of wood density and water content between dry evergreen and dry deciduous forest trees in Central Cambodia. *Japan Agricultural Research Quarterly: JARQ*, 51(4), 363-374.
- 18 Köchy, M., & Wilson, S. D., 2000: Competitive effects of shrubs and grasses in prairie. *Oikos*, 91(2), 385-395.
- 19 Konings, A. G., Piles, M., Rötzer, K., McColl, K. A., Chan, S. K., & Entekhabi, D., 2016: Vegetation optical depth and scattering albedo retrieval using time series of dual-polarized L-band radiometer observations. *Remote sensing of environment*, 172, 178-189.
- 20 Kumar, S. V., Holmes, T., Dharssi, I., Vinodkumar, Hain, C., Peters-Lidard, C., 2020: Characterizing the 2019-2020 Australian bushfires using SMAP vegetation optical depth retrievals, *Geophysical Research Letter (Submitted)*.
- 21 Matthews, S., 2013: Dead fuel moisture research: 1991–2012. *International Journal of Wildland Fire*, 23, 78-92. <https://doi.org/10.1071/WF13005> <https://doi.org/10.1071/WF13005>
- 22 Nelson, R. M., 2001: Water relations of forest fuels. In E. A. Johnson & K. Miyanishi (Eds.), *Forest fires: Behavior and ecological effects*, pp. 79–149, San Diego, California: Academic Press.
- 23 Pellizzaro, G., Cesaraccio, C., Duce, P., Ventura, A., & Zara, P., 2007: Relationships between seasonal patterns of live fuel moisture and meteorological drought indices for Mediterranean shrubland species. *International Journal of Wildland Fire*, 16(2), 232-241.
- 24 Puri, K., Dietachmayer, G., Steinle, P., Dix, M., Rikus, L., Logan, L., ... & Bermous, I., 2013: Implementation of the initial ACCESS numerical weather prediction system. *Australian Meteorological and Oceanographic Journal*, 63, 265-284.
- 25 Qi, Y., Dennison, P. E., Spencer, J., & Riaño, D., 2012: Monitoring live fuel moisture using soil moisture and remote sensing proxies. *Fire Ecology*, 8(3), 71.
- 26 Viegas D. X., Piñol J., Viegas M. T., and Ogaya R., 2001: Estimating live fine fuels moisture content using meteorologically based indices. *International Journal of Wildland Fire*, 10, 223–240.
- 27 Viegas D., Viegas P., and Ferreira A., 1992: Moisture content of fine forest fuels and fire occurrence in central Portugal. *International Journal of Wildland Fire*, 2, 69–85.
- 28 Viney, N. R., 1991: A Review of Fine Fuel Moisture Modelling. *International Journal of Wildland Fire*, 1, 215-234. <https://doi.org/10.1071/WF9910215> <https://doi.org/10.1071/WF9910215>
- 29 Vinodkumar and Dharssi, I., 2017: Evaluation of daily soil moisture deficit used in Australian forest fire danger



- rating system *Bureau of Meteorology Research Reports*, No. 022.
- 30 Vinodkumar and Dharssi, I., 2019: Evaluation and calibration of a high-resolution soil moisture product for wildfire prediction and management. *Agricultural and Forest Meteorology*, 264, 27-39.
 - 31 Vinodkumar, Dharssi, I., Bally, J., Steinle, P., McJannet, D., and Walker, J., 2017: Comparison of soil wetness from multiple models over Australia with observations. *Water Resources Research*, 633-646
 - 32 Williams, K. and Clark, D., 2014: Disaggregation of daily data in JULES, Hadley Centre technical note 96, Hadley Centre, Met Office, UK.
 - 33 Wilson, S. D., 1993: Belowground competition in forest and prairie. *Oikos*, 146-150.
 - 34 Wooster, M. J., Zhukov, B., and Oertel D., 2003: Fire radiative energy for quantitative study of biomass burning: Derivation from the BIRD experimental satellite and comparison to MODIS fire products. *Remote Sensing of the Environment*, 86, 83-107.
 - 35 Xuang, S., 2019: Analysis of the correlation between curing and moisture content in Australian grasslands with MODIS-based observation, Bachelor of Science (Hon.) Thesis (Supervisor: Marta Yebra), Fenner School of Environment and Society, Australian National University, pp119.
 - 36 Yang, Y., Donohue, R. J., & McVicar, T. R., 2016: Global estimation of effective plant rooting depth: Implications for hydrological modeling. *Water Resources Research*, 52(10), 8260-8276.
 - 37 Yebra, M., & Chuvieco, E., 2009: Generation of a species-specific look-up table for fuel moisture content assessment. *IEEE Journal of Selected Topics in Applied Earth Observations and Remote Sensing*, 2(1), 21-26.
 - 38 Yebra, M., & Chuvieco, E., 2009: Linking ecological information and radiative transfer models to estimate fuel moisture content in the Mediterranean region of Spain: Solving the ill-posed inverse problem. *Remote Sensing of Environment*, 113(11), 2403-2411.
 - 39 Yebra, M., Dennison, P. E., Chuvieco, E., Riano, D., Zylstra, P., Hunt Jr, E. R., ... & Jurdao, S., 2013: A global review of remote sensing of live fuel moisture content for fire danger assessment: Moving towards operational products. *Remote Sensing of Environment*, 136, 455-468.
 - 40 Yebra, M., Quan, X., Riaño, D., Larraondo, P. R., van Dijk, A. I., & Cary, G. J., 2018: A fuel moisture content and flammability monitoring methodology for continental Australia based on optical remote sensing. *Remote Sensing of Environment*, 212, 260-272.
 - 41 Yebra, M., Scortechini, G., Badi, A., Beget, M.E., Boer, M.M., Bradstock, R., Chuvieco, E., Danson, F.M., Dennison, P., Resco de Dios, V., Di Bella, C.M., Forsyth, G., Frost, P., Garcia, M., Hamdi, A., He, B., Jolly, M., Kraaij, T., Martín, M.P., Mouillot, F., Newnham, G., Nolan, R.H., Pellizzaro, G., Qi, Y., Quan, X., Riaño, D., Roberts, D., Sow, M., & Ustin, S., 2019: Globe-LFMC, a global plant water status database for vegetation ecophysiology and wildfire applications. *Scientific Data*, 6, 155.